JGR Earth Surface

RESEARCH ARTICLE
10.1029/2020JF005751

Dynamics of Marsh-Derived Sediments in Lagoon-Type Estuaries

Carmine Donatelli[1,2], Tarandeep Singh Kalra[3], Sergio Fagherazzi[4], Xiaohe Zhang[4], and Nicoletta Leonardi[1]

[1]Department of Geography and Planning, School of Environmental Sciences, Faculty of Science and Engineering, University of Liverpool, Liverpool, UK, [2]Department of Estuarine and Delta Systems, Royal Netherlands Institute for Sea Research and Utrecht University, Yerseke, Netherlands, [3]Integrated Statistics, U.S. Geological Survey, Woods Hole Coastal and Marine Science Center, Woods Hole, MA, USA, [4]Department of Earth and Environment, Boston University, Boston, MA, USA

Key Points:
- The sediment eroded from marsh edges helps to build the remaining marshes
- Marsh erosion has a twofold effect: more sediment available for the remaining marshes but decrease in the trapping capacity of the lagoon
- Management actions should consider the effects associated with wetland edge erosion at basin scale

Supporting Information:
- Supporting Information S1

Correspondence to:
C. Donatelli and T. S. Kalra,
carmine.donatelli@nioz.nl;
tkalra@contractor.usgs.gov

Citation:
Donatelli, C., Kalra, T. S., Fagherazzi, S., Zhang, X., & Leonardi, N. (2020). Dynamics of marsh-derived sediments in lagoon-type estuaries. *Journal of Geophysical Research: Earth Surface*, *125*, e2020JF005751. https://doi.org/10.1029/2020JF005751

Received 25 JUN 2020
Accepted 28 SEP 2020
Accepted article online 13 OCT 2020

Author Contributions:
Formal analysis: Carmine Donatelli
Investigation: Carmine Donatelli
Software: Tarandeep Singh Kalra
Writing - original draft: Carmine Donatelli, Tarandeep Singh Kalra, Sergio Fagherazzi, Xiaohe Zhang, Nicoletta Leonardi

Abstract Salt marshes are valuable ecosystems that must trap sediments and accrete in order to counteract the deleterious effect of sea level rise. Previous studies have shown that the capacity of marshes to build up vertically depends on both autogenous and exogenous processes including ecogeomorphic feedbacks and sediment supply from in-land and coastal ocean. There have been numerous efforts to quantify the role played by the sediments coming from marsh edge erosion on the resistance of salt marshes to sea level rise. However, the majority of existing studies investigating the interplay between lateral and vertical dynamics use simplified modeling approaches, and they do not consider that marsh retreat can affect the regional-scale hydrodynamics and sediment retention in back-barrier basins. In this study, we evaluated the fate of the sediments originating from marsh lateral loss by using high-resolution numerical model simulations of Jamaica Bay, a small lagoonal estuary located in New York City. Our findings show that up to 42% of the sediment released during marsh edge erosion deposits on the shallow areas of the basin and over the vegetated marsh platforms, contributing positively to the sediment budget of the remaining salt marshes. Furthermore, we demonstrate that with the present-day sediment supply from the ocean, the system cannot keep pace with sea level rise even accounting for the sediment liberated in the bay through marsh degradation. Our study highlights the relevance of multiple sediment sources for the maintenance of the marsh complex.

1. Introduction

Salt marshes provide critical ecosystem services to coastal communities (Costanza et al., 1997). The economic value of these services has been estimated up to 5 million USD per km^2 in the United States and 1 billion USD per year for all U.K. marshes (Costanza et al., 2008; Leonardi et al., 2017). Salt marshes are inherently unstable along the horizontal direction as they can retreat or expand in response to sediment supply and hydrodynamics (Fagherazzi et al., 2013; Tommasini et al., 2019). Lateral marsh dynamics are strongly related to the rate of sea level rise and to the extension of nearby tidal flats (Fagherazzi et al., 2013; Mariotti & Fagherazzi, 2013a). In fact, waves are locally generated by winds in tidal basins, and large tidal flats increase wave heights and promote high erosion rates (Fagherazzi & Wiberg, 2009). Lateral marsh erosion is recognized as the chief mechanism by which salt marshes are being lost in many estuaries and coastal lagoons around the world (e.g., Marani et al., 2011; Mariotti & Fagherazzi, 2010; Schwimmer, 2001). On the contrary, salt marshes are thought to be stable in the vertical direction due to positive feedbacks between depth of tidal inundation, vegetation biomass production, and sediment trapping efficiency (Marani et al., 2007, 2010; Morris et al., 2002; Pasternack et al., 2000). Projections of coastal wetland response to sea level rise suggest a 20% to 50% reduction of the present-day marsh area by 2100 (Craft et al., 2009; McFadden et al., 2007). These predictions raise concerns about the adaptive capacity of salt marshes to environmental change. Hence, a better understanding of the mechanisms governing salt marsh evolution is crucial to predict the future impact of sea level rise in coastal areas (Orson et al., 1985; Reed, 1995; Stevenson et al., 1985).

Coastal bays must trap sediments to adapt to rising sea level (Fagherazzi et al., 2014; Zhang et al., 2019). Indeed, a positive sediment budget is necessary for the survival of salt marshes and tidal flats

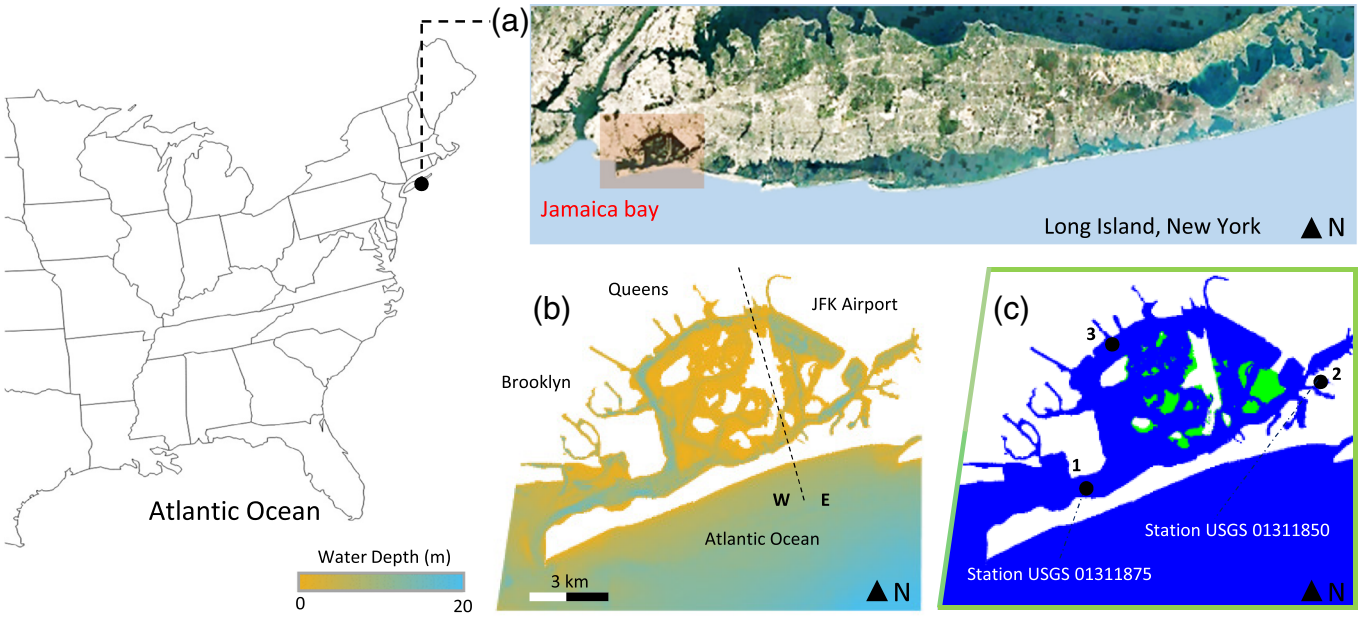

Figure 1. Study area. Long Island (New York City [NYC]) and Jamaica Bay location (a), bathymetry of Jamaica Bay (b), and present-day salt marsh distribution (green areas) and locations of measurements (c). Points 1 and 2 represent the USGS stations (01311875 and 01311850) where water level and SSC data are collected; Point 3 represents the location of the flow velocity measurements; and green lines represent the boundaries of the numerical domain.

(Donatelli, Ganju, Fagherazzi, et al., 2018; Fagherazzi et al., 2014; Ganju et al., 2015). Ganju et al. (2017) demonstrated the existence of a relationship between sediment budget and the unvegetated-vegetated marsh ratio (the unvegetated area consists of ponds, channels, and tidal flats), indicating that sediment deficits are linked to the conversion of vegetated marsh portions into open water. Marsh loss might in turn affect the ability of estuarine systems to retain sediments and cause further deterioration of salt marshes through a positive feedback loop (Donatelli et al., 2020; Donatelli, Ganju, Zhang, et al., 2018). Recent studies indicate that the capacity of salt marshes to keep pace with sea level rise strongly depends on the local tidal range and on the suspended sediment concentration (SSC) in the water that floods the marsh complex during each tidal cycle (Kirwan et al., 2010, 2016). At present, marsh vertical accretion has been rarely analyzed along with horizontal erosional processes (Carniello et al., 2009; Mariotti & Canestrelli, 2017), although the source of sediments generated by edge erosion has been experimentally demonstrated to further increase threshold rates of sea level rise (Ganju et al., 2015; Hopkinson et al., 2018). Simplified marsh-mudflat models have included sediment recycling in salt marsh evolution (e.g., Mariotti & Carr, 2014), but this contribution has been evaluated only in idealized test cases (Mariotti & Canestrelli, 2017). Herein, we use Jamaica Bay as test case to show how the amount of sediments derived from marsh deterioration is redistributed within this highly urbanized estuarine embayment in New York City (USA). We present results of numerical model experiments for the hydrodynamics and sediment transport of Jamaica Bay, using the Coupled-Ocean-Atmosphere-Wave-Sediment Transport (COAWST) modeling system (Warner et al., 2010) and the associated flow-vegetation module (Beudin et al., 2017). A new routine recently implemented in COAWST was used, which explicitly computes marsh lateral erosion based on wave thrust acting on the marsh boundary (Leonardi et al., 2016).

Jamaica Bay watershed hosts more than 2 million people, and its high level of urbanization strongly limits the capacity of this estuary to adapt to external disturbances. Hence, many concerns are rising about the resilience of the bay. The sediment budget of an estuary is an important resilience indicator because it controls the evolution of intertidal areas and their vulnerability to storms and sea level rise. Marine-derived sediment has historically been a crucial component of the sediment budget of the bay (Renfro et al., 2016), but human interventions at Rockaway Inlet have drastically reduced the movement of offshore sediments into the back-barrier basin (Hartig et al., 2002). Peteet et al. (2018) demonstrated, studying two sediment cores taken from marshes located in the eastern and western parts of the bay, that the inorganic fraction is strongly reduced

Table 1
Sediment Characteristics: Sediment Class, Origin, Settling Velocity (mm/s), and Critical Shear Stress for Erosion (N/m^2)

	Sediment class	Origin	Settling velocity (mm/s)	Critical stress for erosion (N/m^2)
1	Medium sand	Bed	40	0.5
2	Fine sand	Bed	5	0.1
3	Silt	Bed	1.5	0.05
4	Mud	Marsh boundary	0.1	0.05
5	Mud	Offshore	0.005	0.05

with respect to the past and only the increase in organic matter flux has allowed Jamaica Bay marshes to keep pace with sea level rise. The lower mineral content due to the reduction in sediment supply has also caused marsh structural weakness and edge failure (Peteet et al., 2018). In this study, we attempt to investigate the fate of the sediments released during marsh edge erosion in Jamaica Bay and analyze the mechanisms governing the sediment dynamics in shallow tidal lagoons.

2. Study Site

Jamaica Bay is a small and highly urbanized coastal lagoon estuary located in Brooklyn, New York City (NYC, Figure 1a). The bay has a total basin area of 50 km^2, with a marsh/basin ratio of ~0.1. The system is connected to the Atlantic Ocean through Rockaway Inlet. The inlet dimensions are limited by the former airport Floyd Bennett Field at the north side and the Rockaway Peninsula at the south side. Waves are locally generated, and tides are mainly semidiurnal, with a mean tidal range of ~1.6 m. The system is flood dominated with a net import of sediment from offshore (Renfro et al., 2016). Deep navigating channels (average depth of 10 m) border the basin, while the central region is shallower and characterized by extensive salt marshes and mudflats (Figure 1b), which provide critical ecosystem services in terms of coastal protection (Marsooli et al., 2017). Furthermore, these wetlands host 324 species of migratory and resident birds and over 90 fish species and are deemed important for horseshoe crabs and diamondback terrapins (New York City Department of Environmental Protection, 2007). As documented by the New York City Department of Environmental Protection (2007), over 75% of salt marshes in Jamaica Bay have been lost since the mid-1800s, and up to a 50% of the marsh deterioration has occurred in the last few decades. The main causes of salt marsh decline have been related to an elevated wave activity associated with ship wakes (Black, 1981; New York City Department of Environmental Protection, 2007), rising sea level (Gornitz et al., 2001; Hartig et al., 2002), increased tidal range (Swanson & Wilson, 2008), and excess nutrients (Wigand et al., 2014). Furthermore, human interventions may have exacerbated marsh loss through alteration of the circulation patterns and sediment budget (Renfro et al., 2016). The present-day salt marsh distribution is depicted in Figure 1c, and *Spartina alterniflora* is the dominant vegetation species in the area.

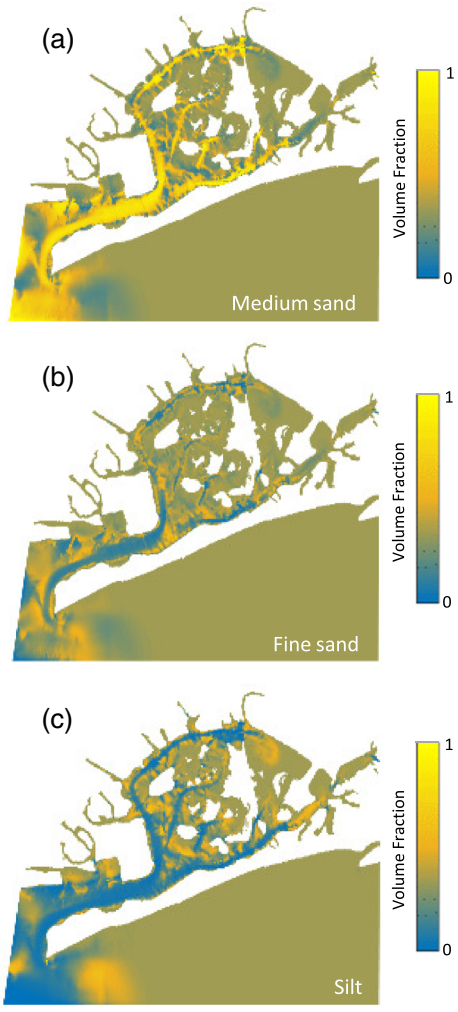

Figure 2. Volume fractions of medium sand (a), fine sand (b), and silt (c) initially distributed on the seabed at the beginning of the simulation.

3. Methods

The hydrodynamics of the system has been simulated using the COAWST modeling framework (Warner et al., 2010). In this study, the circulation model ROMS (Regional Ocean Modeling System) (Shchepetkin & McWilliams, 2005; Warner et al., 2008) and the wave model SWAN (Simulating WAves Nearshore) (Booij et al., 1999) have been fully coupled on the same computational grid. ROMS is a three-dimensional, free surface, finite-difference, terrain following model that solves the Reynolds-

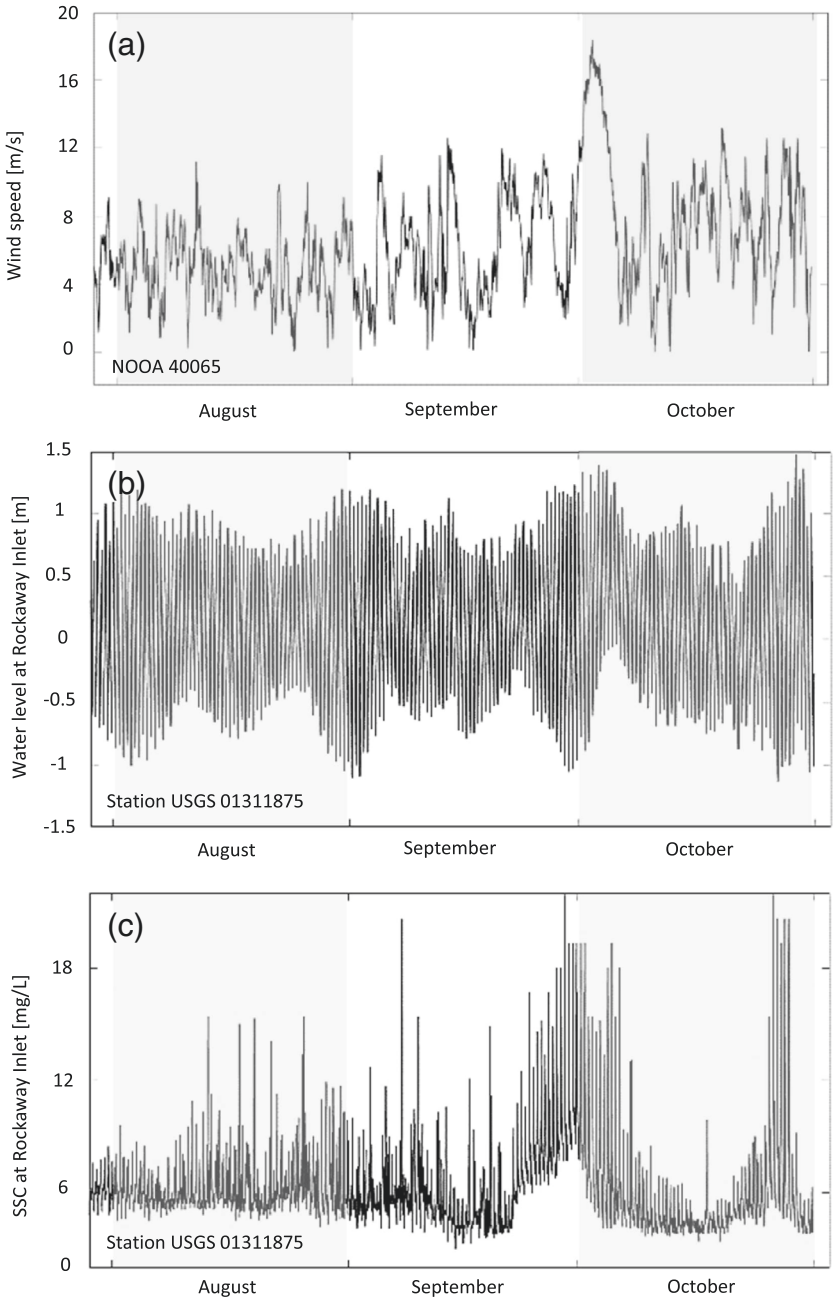

Figure 3. Wind speed (m/s, a), water level (m, b), and SSC (mg/L, c) measurements collected at the NOAA Buoy 44065 and at the inlet mouth between August and October 2015.

averaged Navier-Stokes (RANS) equations using the hydrostatic and Boussinesq assumptions (Haidvogel et al., 2008). SWAN is a third-generation spectral wave model based on the action balance equation (Booij et al., 1999). The model simulates the generation and propagation of wind waves accounting for shifting in relative frequency due to variations in water depth and currents, depth-induced refraction, wave-wave interactions, and dissipation (white capping, depth-induced breaking, and bottom friction). The flow-vegetation interaction is computed by employing the vegetation module implemented by Beudin et al. (2017), which includes plant posture-dependent three-dimensional drag, in-canopy wave-induced streaming, and production and dissipation of turbulent kinetic energy for the vertical mixing parameterization. The spatially averaged vegetation drag force is calculated using a quadratic law, and the

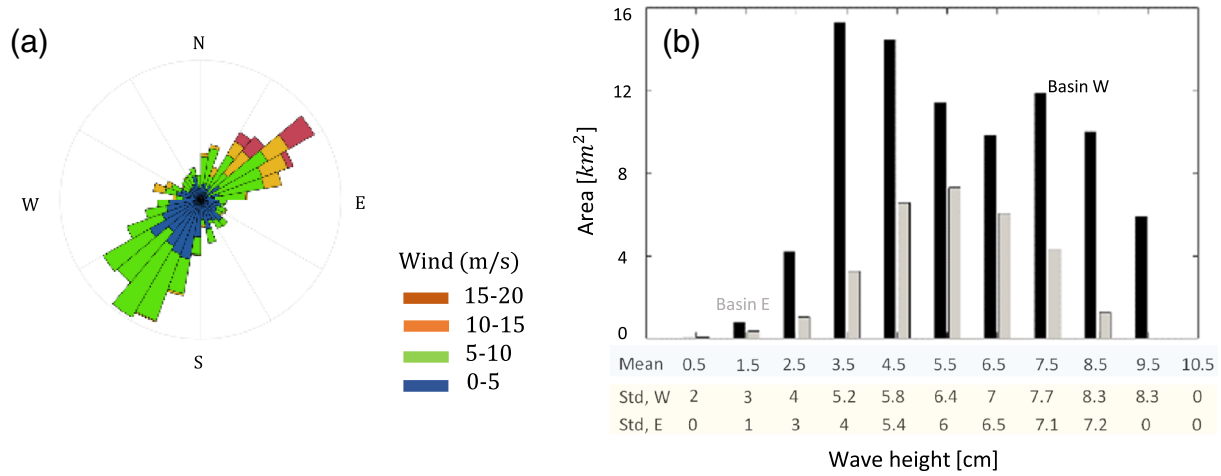

Figure 4. Wind rose for the study area in August–October 2015 (wind station: NOAA Buoy 44065, a); distribution of the mean wave height (cm) and standard deviation (cm) for each subbasin (b). Wave height data are binned every 1 cm.

reduction in drag due to plant flexibility is computed following Luhar and Nepf (2011). The selected turbulence model is the *k*-ε scheme, which accounts for extra dissipation and turbulence kinetic energy production due to vegetation (Uittenbogaard, 2003). Similarly, wave dissipation due to vegetation is accounted for in the model by modifying the source term of the action balance equation following the formulation of Mendez and Losada (2004). The friction exerted by the bed on the flow is computed using a bottom boundary layer formulation (Warner et al., 2008) that includes enhanced wave-based apparent roughness (Madsen, 1994). Wind data are based on observations collected every 6 min at the NOAA Buoy 40065 and applied uniformly on the numerical domain (Figures 3a and 4a).

The number of interior cells is 997 × 387, with cell size varying from 20 to 40 m in the along-bay and cross-bay directions; seven equally spaced layers are defined in the vertical direction. The model is forced at the seaward boundaries with tides, based on observations from the USGS station (USGS 01311875) located at the Rockaway Inlet (Station 1, Figure 1c); a reduction factor is applied to the measured water elevations to consider the effects of convergent topography on the tide when the signal is applied on the boundaries of the numerical domain (Marsooli et al., 2016). The results of the model are compared with water level data collected during 2 weeks in August 2015 at two USGS stations (USGS 01311875 and USGS 01311850, Points 1 and 2 in Figure 1c) and with flow velocities data measured at the North Channel (Point 3, Figure 1c). The model performance is evaluated using root-mean-square error (RMSE), bias, and skill scores (supporting information Table S1). The sediment model incorporates five sediment classes: two noncohesive and three cohesive (Table 1). Cohesive sediment transport is not modeled in ROMS, even though erosion is specified using a flux equation, as it is commonly done for cohesive sediment. Sediment deposition and erosion fluxes at the bottom boundary are formulated as in Warner et al. (2008). One bed layer is implemented with a thickness of 0.25 m and a uniform porosity of 0.5. Three sediment types are initially uniformly distributed over the bed (medium sand, fine sand, and medium silt). A simulation with the initial bed sediment distribution is run for 200 days using only tides. A morphological factor (200) is applied to speed up the sediment dynamics process (e.g., Van der Wegen et al., 2010). Two cohesive sediment classes are used to simulate the material eroded from the marsh boundary (Fagherazzi et al., 2013) and the sediments imported from offshore, respectively (Table 1). The input of sediment coming from the ocean is defined imposing a constant SSC at the western boundary of the numerical domain. The sediment parameters (Table 1) are chosen comparing the modeled signal with the SSC data collected at the USGS station in Rockaway inlet for 2 weeks in August 2015 (Figures S1 and 3c). The modeled SSC time series exhibit a good agreement with measurements (Table S1 and Figure S1). Salt marsh coverage data were derived from the Center for Remote Sensing and Spatial Analysis (CRSSA) geographic information systems database. Vegetation parameters are set as follows: stem height of 0.8 m, diameter of 0.6 cm, and density of 250 shoots/m^2 (Marsooli et al., 2016). A simulation with duration of 80 days (29 July to 16 October 2015) is performed using realistic forcing (e.g., tides and winds) and five sediment classes (Table 1). In this numerical experiment the sediment bed resulting

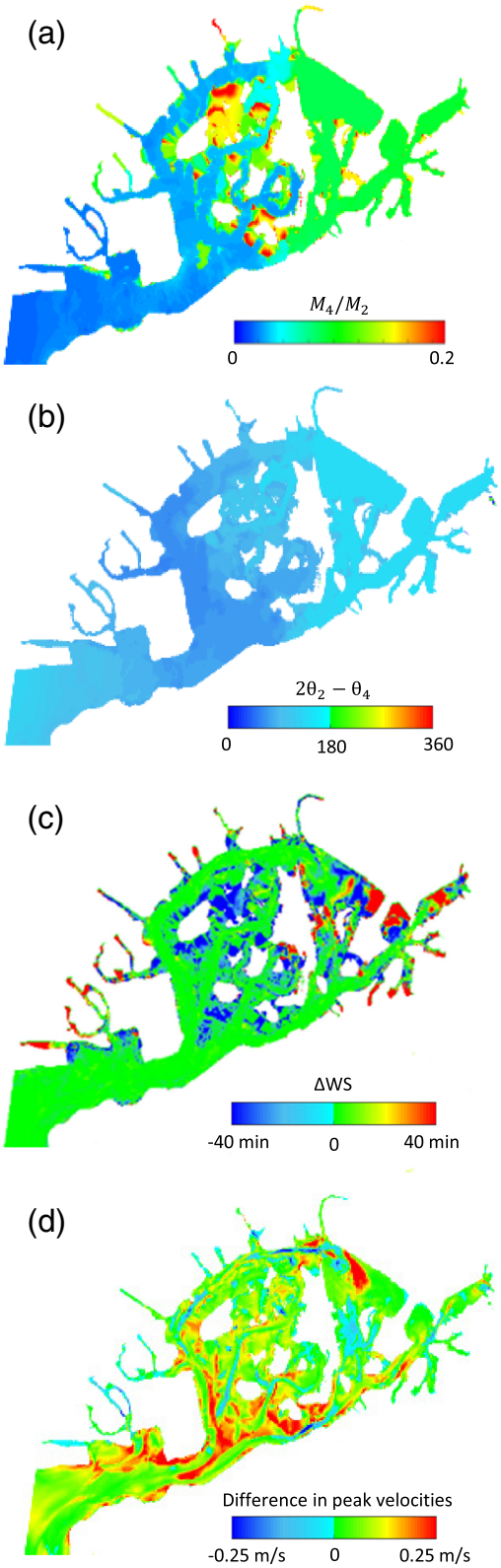

Figure 5. Sea surface amplitude ratio (a) and sea surface phase (b) of M_4 relative to M_2 for the present-day bay morphology. Slack water period asymmetry (min, c) and difference in peak velocities (m/s, d) in Jamaica Bay.

from the 200 day run (Figure 2) is used as initial condition (Ralston et al., 2012). The sediments are classified depending on the location where they are initially released in the numerical domain. For instance, marine-derived materials deposited within the basin are still considered offshore sediments, even though they might be resuspended and trapped by salt marshes during the model's run. To better understand the mechanisms governing the sediment dynamics in Jamaica Bay, an idealized simulation forced only by tides was run for a spring-neap tidal cycle to quantitatively evaluate whether fine sediments (settling velocity = 0.01 mm/s and critical shear stress for erosion = 0.05 Pa) can accumulate in the deep channels bordering the basin until their removal by dredging, or whether these sediments can be reworked and eventually be deposited on marsh platforms as well. More specifically, we defined an initial bed thickness of 0.2 m within the channels of the eastern basin where the bay experiences the lowest shear stress level. In our numerical experiments, we defined as shallow area the entire bay excluding the deep channels bordering the basin.

3.1. Wave Thrust and Marsh Boundary Erosion Calculations

The wave thrust (the integral along the vertical of the dynamic pressure of waves) is explicitly computed by the model following Leonardi et al. (2016) and Tonelli et al. (2010). The total wave thrust (LWT) is given by the sum of two terms:

$$LWT = LWT_{ASL} + LWT_{BSL} \tag{1}$$

The above mean sea level component (LWT_{ASL}) accounts for the hydrostatic pressure from wind waves and is calculated as follows:

$$LWT_{ASL} = 0.5\rho g H_{wave}^2 \tag{2}$$

where ρ is the density of water, g is the acceleration due to gravity, and H_{wave} is the significant wave height. The below sea level component (LWT_{BSL}) accounts for the dynamic pressure of wind waves and includes the effect of changing water level:

$$LWT_{BSL} = \rho g K_p H_{wave} \tag{3}$$

where K_p is the pressure-response factor, and it is computed following Dean and Dalrymple (1991):

$$K_p = \frac{sinh(k(h+\zeta))}{cosh(kh)} \tag{4}$$

where h is the marsh elevation with respect to mean sea level, ζ is the water level, and k is the wave number.

Based on the direction of the waves and grid orientation, the fraction of total thrust that is normal to the marsh-cell face is computed. The effect of water level is considered by reducing exponentially the wave thrust as water level increases above the marsh scarp (Tonelli et al., 2010). After modifying the wave thrust based on water level, the resulting wave thrust from all the cell faces is calculated to obtain a total thrust at each cell center. When the thrust acts on the marsh boundary, marsh erosion takes place generating a sediment bed load on the adjacent cell. The mass of sediment released from marsh cells ($m_{fluxout}$ in kg) depends on wave

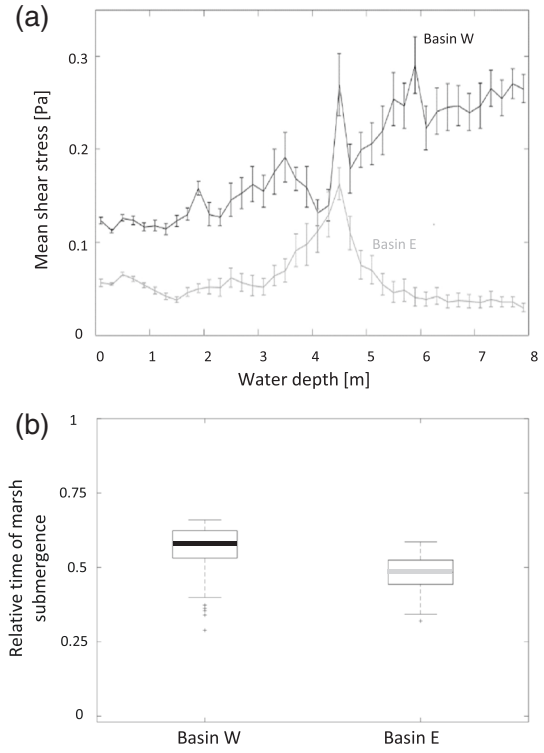

Figure 6. Mean shear stress (Pa) distribution as a function of the water depth (m) for each subbasin (a). Water depth data are binned every 0.2 m. Time of marsh submergence relative to a spring-neap tidal cycle in each subbasin (b).

thrust (LWT in kN/m), a marsh erodibility coefficient (k_{marsh} in s/m), grid size (dx in m), and time step size (dt in s).

$$m_{fluxout} = LWT\ k_{marsh}\ dx\ dt \tag{5}$$

Marsh erosion occurs through a change in bed mass by taking the eroded material from the marsh cell and adding it to the adjacent open-water cell where the wave parameters were computed. The marsh erodibility coefficient, which is inversely proportional to the marsh retreat rate, is chosen to match a marsh erosion rate of 2 m/year. An initial sediment mass was defined over the vegetated surfaces. The sediment parameters are listed in Table 1.

3.2. Evaluation of Tidal Asymmetry

The distortion of the tidal wave is evaluated using the Friedrichs and Aubrey (1988) formulation. Asymmetric tides are important for the transport and deposition of sediment in shallow estuaries (Aubrey & Speer, 1985; Gerkema, 2019). The amplitude and phase ratios between the fourth-diurnal M_4 and the semidiurnal M_2 components were computed within the entire back-barrier basin using T_TIDE (Pawlowicz et al., 2002). The ratio between the amplitude of the overtide and the M_2 component shows the magnitude of the asymmetry, while the relative phase difference ($\varphi = 2 \cdot \vartheta_{M_2} - \vartheta_{M_4}$) reveals the sense of the asymmetry ($0° < \varphi < 180°$: flood dominant; $180° < \varphi < 360°$: ebb dominant; and $\varphi = 0°, 180°$: symmetric tidal wave). An examination of slack duration and maximum velocity is performed following Dronkers (1986). An asymmetry in the slack water periods may affect the residual transport of fine sediments, while a difference in the peak velocities during ebb and flood may influence the residual transport of coarse material. Flood-dominant slack-period asymmetry occurs when the time derivative of the velocity at high water is smaller than the velocity variation at low water. The water slack period has been defined as the time where the depth-averaged flow velocity is below the critical value proposed by Vermeulen (2003). The average periods of high (HWS) and low (LWS) slack water have been calculated for the entire bay for a spring-neap tidal cycle and used to compute the tidal averaged slack water dominance ($\Delta WS = HWS - LWS$). A positive ΔWS value indicates that fine sediments have a longer time to deposit during the slack period after the flood phase than after the ebb phase.

3.3. Estimation of Sediment Budget

The minimum sediment supply (B) required for the entire bay to keep pace with sea level rise can be calculated as follows (Chant et al., 2020; Ganju et al., 2020):

$$B = slr\ (A_m \rho_m + As_b \rho s_b) \tag{6}$$

where slr is the rate of sea level rise, ρ_m and ρs_b are the bulk densities for marshes and subtidal areas, and A_m and As_b represent the marsh extent and the subtidal area. The local sea level rise is estimated following assessments based on monthly mean sea level observations taken at The Battery (New York) in the period

Table 2
Fate of marine-derived sediments within Jamaica Bay after 80 days. Values (i,j) in the table indicate the percentage of sediments stored on salt marshes, shallow areas, and deep channels with respect to the sediment imported into the bay. The sediment mass imported from offshore is 2.0 x 10^6 kg/month.

	Deposition/Trapping			Suspension	
	Marshes	Shallow areas	Deep channels	Shallow areas	Deep channels
W-B	1%	43%	6.4%	15.8%	10%
E-B	0.6%	12.8%	2.6%	4.5%	3%

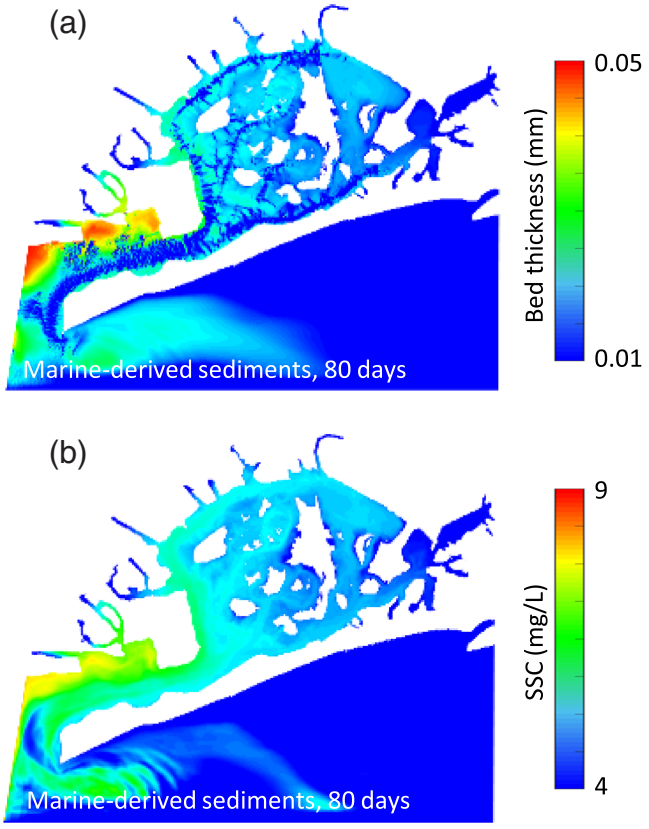

Figure 7. Sediment deposition (a) and suspended sediment concentrations (b) after 80 days (marine-derived sediments only).

1856–2019. These measurements, available on the NOAA site, show a local relative sea level trend of 2.87 mm/year with a 95% confidence interval of ±0.09 mm/year. Studies based on more recent periods demonstrate how sea level trend has been accelerating in this region, estimating rates of sea level rise up to 4.70 mm/year (e.g., Miller et al., 2013). Bulk density values are chosen following Morris et al. (2016) for marshes (373 ± 214 kg/m^3) and Renfro et al. (2010) for subtidal areas (700 kg/m^3). Table S2 depicts the values of the parameters in Equation 6.

4. Results

The convergent shape of the inlet increases tides in the bay resulting in water oscillations greater than the offshore tidal amplitude (Aretxabaleta et al., 2014). The tidal wave experiences a distortion due to the basin morphology, altering its symmetric shape. The system is flood dominated as showed in Figure 5. The sea-surface phase (Figure 5b) is between 0° and 180° within the entire system, and the rate of tidal distortion increases from the mouth to the interior part of the estuary, with peaks over the shallow area in the central part of the basin (Figure 5a). Furthermore, our findings demonstrate how the asymmetry in the slack water duration is pronounced only in shallow areas of the basin, while in the deep channels, it is negligible (Figure 5c). Figure 5d presents the difference in the depth-averaged peak velocity currents during the flood and ebb phases; this result is in agreement with Figure 5b and shows the overall flood dominance of the estuary, although this behavior is not observed in the areas of the basin where water depth exceeds 8 m. This discrepancy is attributed to the fact that the Friedrichs and Aubrey (1988) formulation is built for shallow well-mixed channels/estuaries. Furthermore, comparing the asymmetry in tidal velocity for different parts of the water column might give a better metric of flood/ebb dominance and its influence on sediment transport.

The distribution of mean bottom shear stress as a function of water depth shows that in the western part of the basin bottom shear stresses increase monotonically with water depth, while intermediate water depths experience the maximum value in bottom shear stress in the eastern part of the estuary (Figure 6a). The two subbasins have different fetch values and therefore different wave heights (Figure 4b). The peak in shear stress distribution in the eastern part of the basin is related to the fact that shear stresses are limited both in shallower areas because of dissipative processes and in deeper areas because the bottom is too deep to be affected by wind waves (Fagherazzi et al., 2006). Figure 6b shows the time of marsh submergence in each subbasin. Marshes located in the eastern subbasin have a shorter time of submergence and consequently a shorter time to trap sediments during each tidal cycle.

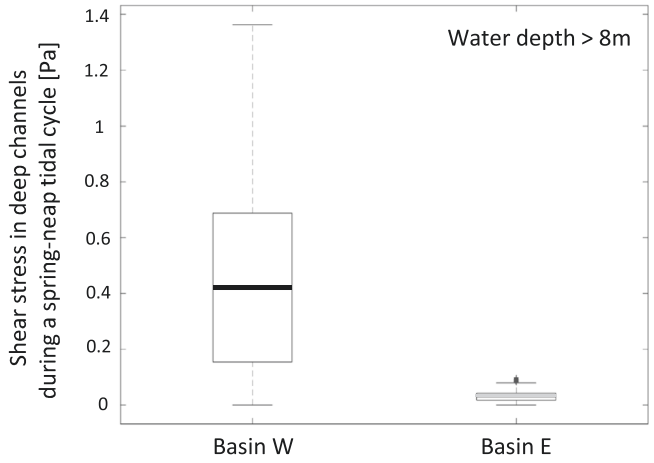

Figure 8. Variability of shear stress in deep channels during a spring-neap tidal cycle.

Table 2 depicts how marine-derived sediments are distributed over the subtidal flats after 80 days. This table shows that a big fraction of the sediment coming from offshore is trapped by the western subbasin. Indeed, lower sediment concentrations and deposition are observed in the eastern part of the system. Spatial distributions of sediment deposition and SSCs are shown in Figures 7a and 7b, respectively. Table 2 presents how offshore sediments are stored in the bay and shows that only a small fraction (<2%) deposit over salt marshes, although more than 35% of this sediment mass is kept in suspension and remains available to be potentially trapped

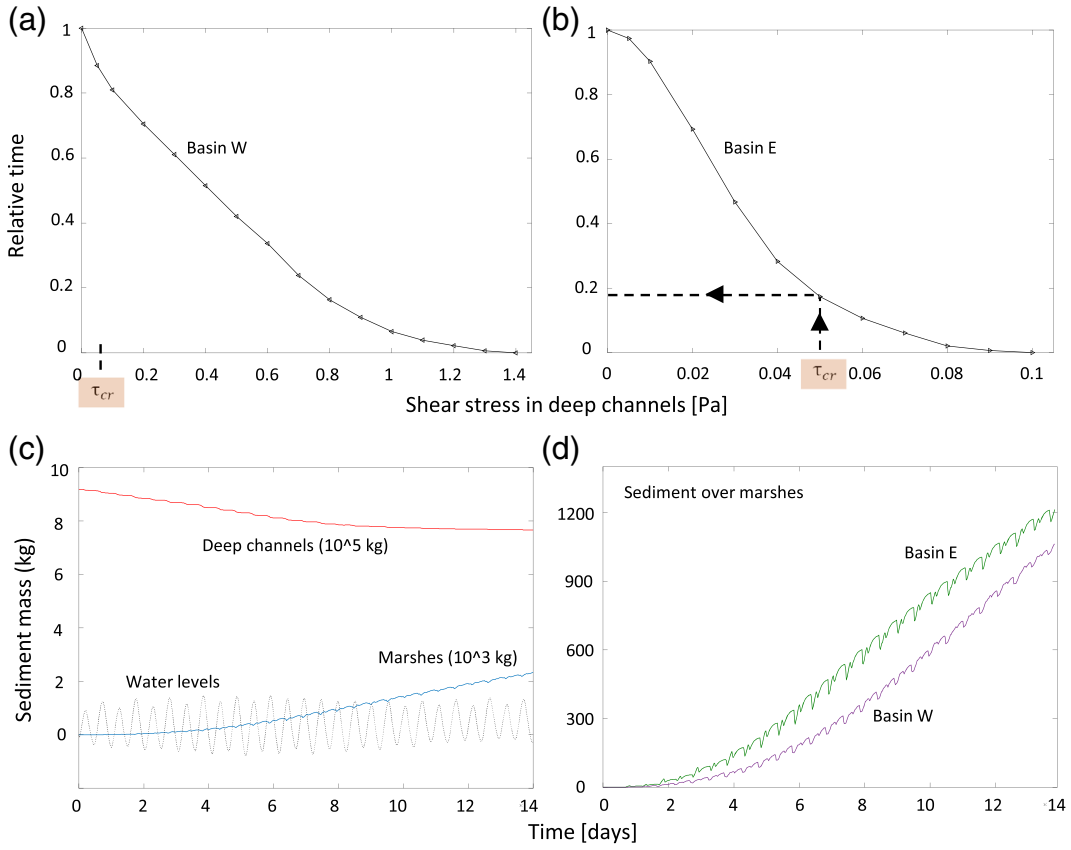

Figure 9. Relative time in a spring-neap tidal cycle in which shear stresses are higher of a certain value in the western (a) and eastern (b) subbasins. Time seriesof the sediment mass in deep channels (c) and over salt marsh platforms (d).

by vegetation at a later time. Furthermore, we evaluated the average sediment mass imported from offshore in a month as 2×10^6 kg.

The box plot of shear stresses induced by only tides, calculated in a spring-neap tidal cycle, shows that the deep channels in the eastern subbasin are more likely to serve as potential sediment sinks given their low shear stress levels (Figure 8). Figure 9b demonstrates that shear stresses are higher or equal to 0.05 Pa for the 18% of the spring-neap tidal cycle during which silt and mud can be resuspended and potentially trapped

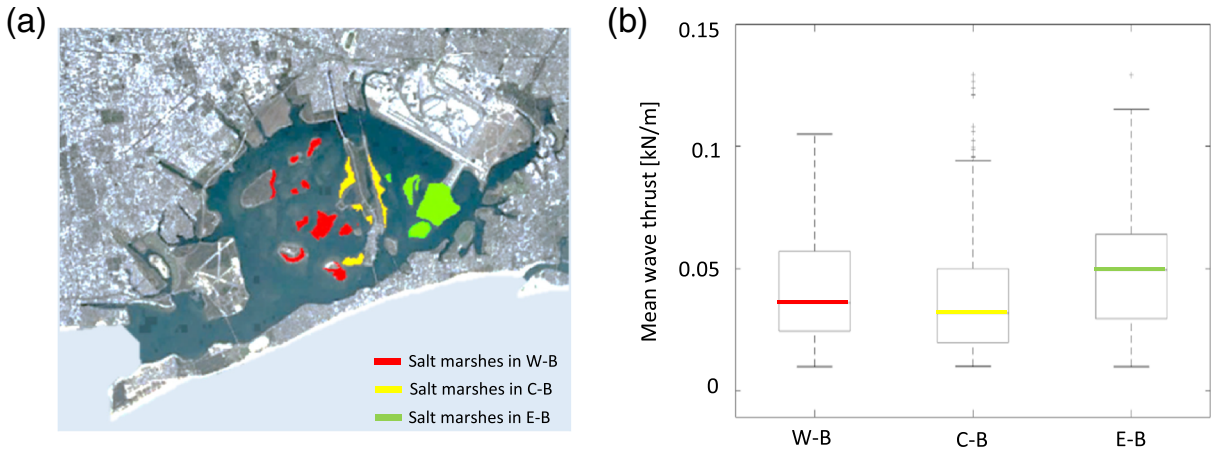

Figure 10. Marsh location in the basin (W-B = western subbasin; CB= central subbasin; E-B = eastern subbasin, a); wave thrust values (kN/m) for each group (b).

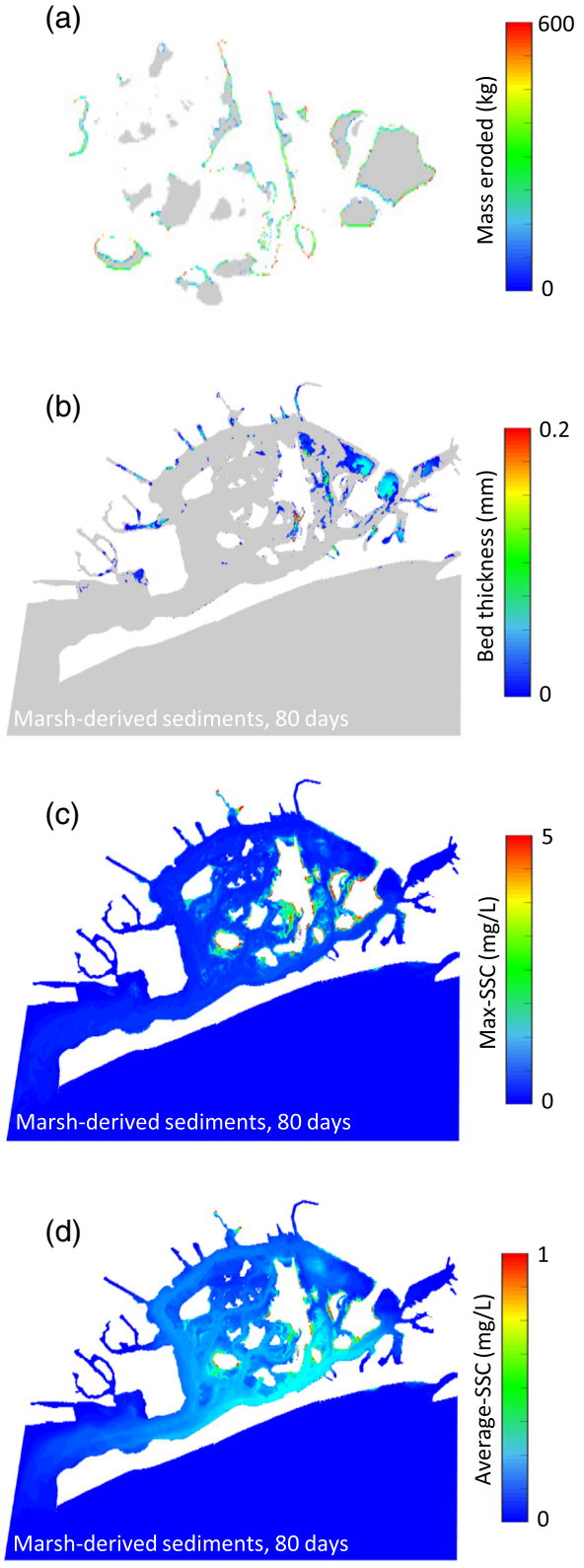

Figure 11. Fate of marsh-derived sediments within the estuary after 80 days. Values (i,j) in the table indicate the percentage of sediments stored on salt marshes,shallow areas, and deep channels with respect to the total mass of sediments released by wave-induced lateral erosion.

by salt marshes in the eastern subbasin. We computed the sediment mass stored over marshes and the mass still present in the channels (given the setup in the idealized simulations, no other sediments can be remobilized except those in the channels). Our numerical experiment shows that fine sediments deposited in deep channels can be remobilized during spring tides (Figure 9c) and trapped in salt marshes (Figure 9d). It is worth noticing that the sediment deposition is higher over the salt marshes in the eastern subbasin, because the initial bed thickness was defined only within the channels of the eastern part of the bay.

The impact of wind waves along the marsh boundaries is evaluated in terms of wave thrust per unit width. The average wave thrust for the period August–October 2015 is depicted in Figure 10 for marshes located in the western (W-B), central (C-B), and eastern (E-B) part of the bay. The variability of the averaged wave thrust is higher in the eastern subbasin, while the mean wave thrust is lower for salt marshes located in the central part of the bay. However, differences are not significant. Figure 11a shows the simulated mass eroded from salt marshes in 80 days. As the shear stresses are higher in the western part of the basin (Figure 6a), sediment deposition over the shallow area is very limited and marsh-derived sediments are trapped more efficiently by the vegetated surfaces (Figure 11b). On the contrary, the sediments eroded from salt marshes mainly deposit over the shallow area in the eastern subbasin (Figure 11b). The remaining sediment is kept in suspension by waves and tides in the water column or lost to the ocean. Figures 11c and 11d present maximum and average values of SSCs over the last tidal cycle, respectively. These figures show how the sediment eroded from salt marshes is distributed rapidly within the entire basin. Table 3 summarizes these results and shows that 19% of the sediment released by salt marshes during edge erosion (1.0×10^5 kg/month) is trapped by vegetated surfaces. Around 50% of the eroded material deposits over the vegetated surfaces, deep channels, and shallow parts of the bay. The remaining fraction is lost to the ocean. Furthermore, our numerical experiments revealed that offshore and marsh-derived sediments contribute almost equally to marsh vertical accretion (32×10^3 and 19×10^3 kg/month, respectively).

5. Discussion

In this study, we aim to highlight the relative contribution of different sediment sources to the accretion rate of salt marshes by focusing on sediments derived from salt marsh erosion. Results are based on a linear relationship between wave thrust acting on marsh edges and the amount of sediment liberated in the basin through marsh retreat (Leonardi & Fagherazzi, 2014). A shortcoming of this modeling approach is related to the choice to use a uniform marsh erodibility coefficient for the entire domain (Equation 5). In reality, this coefficient can vary widely in coastal settings depending on the local shoreline characteristics (Schwimmer, 2001). Furthermore, the marsh erodibility coefficient is a fixed user input. In this test case, we chose the coefficient based on a marsh retreat of 2 m/year, which is consistent with marsh erosion rates in Jamaica Bay (Hartig et al., 2002).

Table 3
Sediment eroded from marsh boundary (kg) after 80 days (a). Sediment deposition (b), maximum suspended sediment concentrations (c), and average suspended sediment concentrations (d) over the last tidal cycle (only marsh-derived sediments). The sediment mass liberated through marsh lateral erosion is 1.0 x 10^5 kg/month.

	Deposition/Trapping			Suspension	
	Marshes	Shallow areas	Deep channels	Shallow areas	Deep channels
W-B	12%	5%	1%	5%	1.7%
E-B	7%	18%	7%	1.5%	1%

Our findings (Figure 11 and Table 3) show that up to 42% of the sediment released from marshes during edge erosion deposits on the shallow areas of the basin (23%) or is trapped by vegetated surfaces (19%). Moreover, as the system is flood dominated (Figure 5), the stronger tidal currents during the flood phase favor the retention of the sediment coming from marsh deterioration, increasing the sediment supplied to the remaining salt marshes. Long-term numerical simulations would provide a comprehensive view of how marsh-derived sediments are redistributed within the estuary under a wider range of forcings and allow us to better understand the interplay between marsh lateral erosion and marsh vertical accretion. Indeed, interseasonal and interannual variability in the wind field could drive large changes in the sediment transport in back-barrier estuaries (e.g., Duran-Matute et al., 2016).

Recent outcomes indicate that the resilience of salt marshes is linked not only to the sediment budget of the vegetated surfaces but also of surrounding tidal flats, sea bed, and tidal channels (Fagherazzi, 2014; Lauzon et al., 2018). Therefore, even though 23% of sediments deposit on the shallow areas of the basin, our findings suggest that marsh-derived sediment can increase the resistance of salt marshes to sea level rise by contributing to the marsh sediment budget, in agreement with previous works (Ganju et al., 2015; Hopkinson et al., 2018).

As suggested by Mariotti and Fagherazzi (2013b), the equilibrium depth of tidal flats is defined by a balance between erosion from wave-generated shear stress and deposition proportional to sediment concentration, modulated by sea level rise. Hence, accumulation of sediments released during marsh edge erosion over shallow areas may reduce their depth, inducing subsequent erosion and higher suspended sediment concentrations in the water column. Since the suspended sediment in the water column increases, the efficiency of salt marshes in trapping sediments generated by their own degradation might raise once changes in bathymetry associated with the deposition of marsh-derived sediments become important (Figure 12).

Several insightful studies have investigated the resistance of salt marshes to sea level rise under different sediment supply conditions. However, many of these studies use simplified approaches prescribing constant suspended sediment concentration and do not account for the hydromorphodynamic feedbacks regulating the redistribution of sediments derived from the erosion of marsh boundaries (Kirwan et al., 2010; Morris et al., 2002). For example, Kirwan et al. (2010) estimate threshold rates of sea level rise by imposing various suspended sediment values, ignoring the origin of the sediment, their spatiotemporal variability, and the impact of marsh disappearance on the regional-scale hydrodynamics (Donatelli, Ganju, Zhang, et al., 2018; Ganju et al., 2015; Hopkinson et al., 2018). We have demonstrated that salt marsh resistance to sea level rise can benefit from marsh degradation as the latter can contribute to the local sediment budget, albeit in this specific test case marsh lateral erosion results in loss of habitat, as salt marshes cannot migrate landward given the high level of urbanization of the watershed.

Although salt marsh erosion would positively affect the sediment budget of the marsh complex in the short term (marsh erosion does not alter significantly the estuarine morphology and in particular the marsh/basin area ratio), the increase in the flushing capacity of the system associated with extensive marsh loss might compromise the fate of the estuary, and marshes themselves, over long timescales (when changes in estuarine morphology induced by marsh loss significantly modify the hydrodynamics of the back-barrier basin) (Donatelli et al., 2020). Indeed, large-scale marsh deterioration increases the intertidal storage volume of the back-barrier basin, fetch values, and bottom shear stresses, reducing the sediment stock in the entire system. As a consequence, the sediment trapping capacity of marsh platforms decreases nonlinearly with marsh decline, and this may reduce their ability to counteract sea level rise even accounting for sediment recycling (Donatelli et al., 2020; Donatelli, Ganju, Zhang, et al., 2018). In the long term, changes in sediment

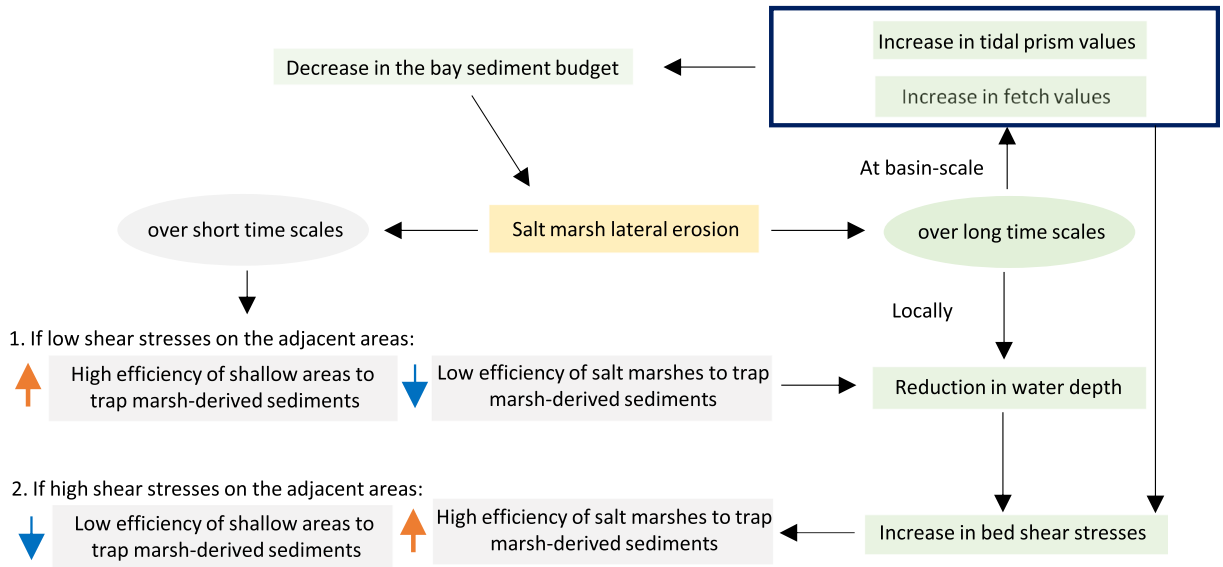

Figure 12. Efficiency of salt marshes in trapping marsh-derived sediment over short and long timescales.

availability associated with marsh loss might also influence erosional processes. More specifically, a simplified model proposed by Mariotti and Fagherazzi (2013a) demonstrates that the ratio between marsh and open-water area in a bay is controlled by the amount of sediment stored within the basin, showing how sea level rise can speed up marsh lateral erosion by reducing the overall sediment storage. Moreover, lower marsh to open water ratios might trigger a positive feedback loop with further marsh deterioration (Mariotti & Carr, 2014; Tambroni & Seminara, 2012), but erosion rates would decrease with the widening of tidal flats (Mariotti & Canestrelli, 2017). The interplay between marsh erosion and sediment trapping on marsh platforms might be also influenced by the bottom characteristics of the basin. As proposed by the exploratory model of Donatelli et al. (2019), submerged aquatic vegetation reduces wave thrust values along marsh boundaries and alters the sediment exchange between tidal flats and marshes, enhancing deposition on vegetated beds rather than resuspension and deposition on marsh platforms (Donatelli, Ganju, Fagherazzi, et al., 2018; Nardin et al., 2018). Our research underlines the role of autogenous processes on the stability and evolution of salt marshes and determines the fate of the sediments derived from marsh edge erosion in shallow estuaries.

6. Conclusions

Marine-derived sediments represent an important sediment source to Jamaica Bay, contributing significantly to the elevation gain of marshes and tidal flats. However, human interventions at the inlet have dramatically decreased the sediment supply from offshore (Hartig et al., 2002) and altered the physical response of the back-barrier basin to tides and low-frequency disturbances (e.g., Orton et al., 2015; Talke & Jay, 2020). Using a numerical modeling approach, we quantified the sediment flux at the mouth of the estuary, evaluating the fate of sediments within the bay (Table 2 and Figure 7). Our findings show a strong agreement with previous sediment budget estimations carried out by Chant et al. (2020) and Renfro et al. (2016).

A simplified approach based on Equation 6 indicates that the sediment necessary for the estuary to keep pace with sea level rise (~8×10^6 kg/month: 0.38×10^6 kg/month for marshes and 7.62×10^6 kg/month for subtidal areas) is larger than the present-day supply of sediment from the ocean estimated in this study (~2×10^6 kg/month). However, our analysis may underestimate the actual sediment mass imported from offshore, as we do not consider the effect of storm surges (e.g., Castagno et al., 2018). This study demonstrates that sediments liberated in the basin through marsh degradation are not sufficient to offset the deficit of the entire system. Nevertheless, we argue that marsh erosion can play an important role in limiting the disappearance of the remaining salt marshes with rising sea level. Indeed, we revealed that the net sediment eroded from marshes (1.0×10^5 kg/month) is trapped mainly by vegetated surfaces and shallow areas,

positively contributing to the sediment budget of the marsh complex. From a management perspective, we conclude that (1) protection of marsh edges from lateral retreat would decrease the sediment released through lateral erosion, further compromising salt marshes under future sea level rise scenarios. Nevertheless, without protection, salt marshes will disappear due to lateral erosion, and therefore, further studies are necessary to evaluate the best solution to preserve this vegetated ecosystem. (2) The new marsh erosion modeling routines of COAWST provide an important tool for coastal managers: It can localize potential hotspots of marsh degradation and might help prioritize investments. (3) Management actions should be evaluated at the basin scale, by taking into account natural physical processes associated with wetland edge erosion, and sedimentation/erosion on tidal flats and main channels.

Data Availability Statement

Data are available online (https://zenodo.org/deposit?page=1&size=20).

Acknowledgments

This study was supported by the Department of the Interior Hurricane Sandy Recovery program (ID G16AC00455, subaward to University of Liverpool). S. F. was partly supported by NSF awards 1637630 (PIE LTER) and 1832221 (VCR LTER). We thank Robert Chant from Rutgers University for sharing the hydrodynamic measurements in Jamaica Bay. We thank the Editor, F. Grasso, Brad Murray, and the two anonymous reviewers for critical revision of the manuscript.

References

Aretxabaleta, A. L., Butman, B., & Ganju, N. K. (2014). Water level response in back-barrier bays unchanged following Hurricane Sandy. *Geophysical Research Letters*, *41*, 3163–3171. https://doi.org/10.1002/2014GL059957

Aubrey, D. G., & Speer, P. E. (1985). A study of non-linear tidal propagation in shallow inlet estuarine systems. Part I. Observations. *Estuarine, Coastal and Shelf Science*, *21*(2), 185–205. https://doi.org/10.1016/0272-7714(85)90096-4

Beudin, A., Kalra, T. S., Ganju, N. K., & Warner, J. C. (2017). Development of a coupled wave-flow vegetation interaction model. *Computers and Geosciences*, *100*, 76–86. https://doi.org/10.1016/j.cageo.2016.12.010

Black, F. R. (1981). *Jamaica Bay: A history. Cultural resource management study 3*. Washington, DC: Natl Park Serv.

Booij, N., Ris, R. C., & Holthuijsen, L. H. (1999). A third-generation wave model for coastal regions: I. Model description and validation. *Journal of Geophysical Research*, *104*(C4), 7649–7666. https://doi.org/10.1029/98JC02622

Carniello, L., Defina, A., & D'Alpaos, L. (2009). Morphological evolution of the Venice lagoon: Evidence from the past and trend for the future. *Journal of Geophysical Research 114*, F04002 https://doi.org/10.1029/2008JF001157

Castagno, K. A., Jiménez-Robles, A. M., Donnelly, J. P., Wiberg, P. L., Fenster, M. S., & Fagherazzi, S. (2018). Intense storms increase the stability of tidal bays. *Geophysical Research Letters*, *45*, 5491–5500. https://doi.org/10.1029/2018GL078208

Chant, R. J., Ralston, D. K., Ganju, N. K., Pianca, C., Simonson, A. E., & Cartwright, R. A. (2020). Sediment budget estimates for a highly impacted embayment with extensive wetland loss. *Estuaries and Coasts*. https://doi.org/10.1007/s12237-020-00784-3

Costanza, R., d'Arge, R., de Groot, R. S., Farber, S., Grasso, M., Hannon, B., et al. (1997). The value of the world's ecosystem services and natural capital. *Nature*, *387*(6630), 253–260. https://doi.org/10.1038/387253a0

Costanza, R., Perez-Maqueo, O., Martinez, M. L., Sutton, P., Anderson, S. J., & Mulder, K. (2008). The value of coastal wetlands for hurricane protection. *Ambio*, *37*(4), 241–248. https://doi.org/10.1579/0044-7447(2008)37[241:TVOCWF]2.0.CO;2

Craft, C., Clough, J., Ehman, J., Joye, S., Park, R., Pennings, S., et al. (2009). Forecasting the effects of accelerated sea-level rise on tidal marsh ecosystem services. *Frontiers in Ecology and the Environment*, *7*(2), 73–78. https://doi.org/10.1890/070219

Dean, R. G., & Dalrymple, R. A. (1991). *Water wave mechanics for engineers and scientists* (p. 353). Singapore: World Sci.

Donatelli, C., Ganju, N. K., Fagherazzi, S., & Leonardi, N. (2018). Seagrass impact on sediment exchange between tidal flats and salt marsh, and the sediment budget of shallow bays. *Geophysical Research Letters*, *45*, 4933–4943. https://doi.org/10.1029/2018GL078056

Donatelli, C., Ganju, N. K., Kalra, T., Fagherazzi, S., & Leonardi, N. (2019). Changes in hydrodynamics and wave energy as a result of seagrass decline along the shoreline of a microtidal back-barrier estuary. *Advances in Water Resources*, *128*, 183–192. https://doi.org/10.1016/j.advwatres.2019.04.017

Donatelli, C., Ganju, N. K., Zhang, X., Fagherazzi, S., & Leonardi, N. (2018). Salt marsh loss affects tides and the sediment budget of shallow bays. *Journal of Geophysical Research: Earth Surface*, *123*, 2647–2662. https://doi.org/10.1029/2018JF004617

Donatelli, C., Zhang, X., Ganju, N. K., Aretxabaleta, A. L., Fagherazzi, S., & Leonardi, N. (2020). A nonlinear relationship between marsh size and sediment trapping capacity compromises salt marshes' stability. *Geology*, *48*(10), 966–970. https://doi.org/10.1130/G47131.1

Dronkers, J. (1986). Tidal asymmetry and estuarine morphology. *Netherlands Journal of Sea Research*, *20*(2–3), 117–131. https://doi.org/10.1016/0077-7579(86)90036-0

Duran-Matute, M., Gerkema, T., & Sassi, M. (2016). Quantifying the residual volume transport through a multiple-inlet system in response to wind forcing: The case of the western Dutch Wadden Sea. *Journal of Geophysical Research: Oceans*, *121*, 8888–8903. https://doi.org/10.1002/2016JC011807

Fagherazzi, S. (2014). Coastal processes: Storm-proofing with marshes. *Nature Geoscience*, *7*(10), 701–702. https://doi.org/10.1038/ngeo2262

Fagherazzi, S., Carniello, L., D'Alpaos, L., & Defina, A. (2006). Critical bifurcation of shallow microtidal landforms in tidal flats and salt marshes. *Proceedings of the National Academy of Sciences of the United States of America*, *103*(22), 8337–8341. https://doi.org/10.1073/pnas.0508379103

Fagherazzi, S., Mariotti, G., Wiberg, P. L., & McGlathery, K. J. (2013). Marsh collapse does not require sea level rise. *Oceanography*, *26*(3), 70–77. https://doi.org/10.5670/oceanog.2013.47

Fagherazzi, S., Mariotti, G., Wiberg, P. L., & McGlathery, K. J. (2014). Marsh collapse does not require sea level rise. *Oceanography*, *26*(3), 70–77. https://doi.org/10.5670/oceanog.2009.80

Fagherazzi, S., & Wiberg, P. L. (2009). Importance of wind conditions, fetch, and water levels on wave-generated shear stresses in shallow intertidal basins. *Journal of Geophysical Research*, *114*, F03022. https://doi.org/10.1029/2008JF001139

Friedrichs, C. T., & Aubrey, D. G. (1988). Non-linear tidal distortion in shallow well-mixed estuaries: A synthesis. *Estuarine, Coastal and Shelf Science*, *27*(5), 521–545. https://doi.org/10.1016/0272-7714(88)90082-0

Ganju, N. K., Defne, Z., & Fagherazzi, S. (2020). Are elevation and open-water conversion of salt marshes connected? *Geophysical Research Letters*, *47*, e2019GL086703. https://doi.org/10.1029/2019GL086703

Ganju, N. K., Defne, Z., Kirwan, M. L., Fagherazzi, S., D'Alpaos, A., & Carniello, L. (2017). Spatially integrative metrics reveal hidden vulnerability of microtidal salt marshes. *Nature Communications*, *8*, p.ncomms14156.

Ganju, N. K., Kirwan, M. L., Dickhudt, P. J., Guntenspergen, G. R., Cahoon, D. R., & Kroeger, K. D. (2015). Sediment transport-based metrics of wetland stability. *Geophysical Research Letters*, *42*, 7992–8000. https://doi.org/10.1002/2015GL065980

Gerkema, T. (2019). *An introduction to tides*. Cambridge: Cambridge University Press. https://doi.org/10.1017/9781316998793

Gornitz, V., Couch, S., & Hartig, E. K. (2001). Impacts of sea level rise in the New York City metropolitan area. *Global and Planetary Change*, *32*(1), 61–88. https://doi.org/10.1016/S0921-8181(01)00150-3

Haidvogel, D. B., Arango, H., Budgell, W. P., Cornuelle, B. D., Curchitser, E., Di Lorenzo, E., et al. (2008). Regional ocean forecasting in terrain-following coordinates: Model formulation and skill assessment. *Journal of Computational Physics*, *227*, 3595–3624.

Hartig, E. K., Gornitz, V., Kolker, A., Mushacke, F., & Fallon, D. (2002). Anthropogenic and climate-change impacts on salt marshes of Jamaica Bay, New York City. *Wetlands*, *22*(1), 71–89. https://doi.org/10.1672/0277-5212(2002)022[0071:AACCIO]2.0.CO;2

Hopkinson, C. S., Morris, J. T., Fagherazzi, S., Wollheim, W. M., & Raymond, P. A. (2018). Lateral marsh edge erosion as a source of sediments for vertical marsh accretion. *Journal of Geophysical Research: Biogeosciences*, *123*, 2444–2465. https://doi.org/10.1029/2017JG004358

Kirwan, M. L., Guntenspergen, G. R., D'Alpaos, A., Morris, J. T., Mudd, S. M., & Temmerman, S. (2010). Limits on the adaptability of coastal marshes to rising sea level. *Geophysical Research Letters*, *37*, L23401. https://doi.org/10.1029/2010GL045489

Kirwan, M. L., Temmerman, S., Skeehan, E. E., Guntenspergen, G. R., & Fagherazzi, S. (2016). Overestimation of marsh vulnerability to sea level rise. *Nature Climate Change*, *6*(3), 253–260. https://doi.org/10.1038/nclimate2909

Lauzon, R., Murray, A. B., Moore, L. J., Walters, D. C., Kirwan, M. L., & Fagherazzi, S. (2018). Effects of marsh edge erosion in coupled barrier island-marsh systems and geometric constraints on marsh evolution. *Journal of Geophysical Research: Earth Surface*, *123*, 1218–1234. https://doi.org/10.1029/2017JF004530

Leonardi, N., Carnacina, I., Donatelli, C., Ganju, N. K., Plater, A. J., Schuerch, M., & Temmerman, S. (2017). Dynamic interactions between coastal storms and salt marshes: A review. *Geomorphology*, *301*, 92–107.

Leonardi, N., Defne, Z., Ganju, N. K., & Fagherazzi, S. (2016). Salt marsh erosion rates and boundary features in a shallow Bay. *Journal of Geophysical Research: Earth Surface*, *121*, 1861–1875. https://doi.org/10.1002/2016JF003975

Leonardi, N., & Fagherazzi, S. (2014). How waves shape salt marshes. *Geology*, *42*(10), 887–890. https://doi.org/10.1130/G35751.1

Luhar, M., & Nepf, H. (2011). Flow induced reconfiguration of buoyant and flexible aquatic vegetation. *Limnology and Oceanography*, *56*(6), 2003–2017.

Madsen, O. S. (1994). Spectral wave–current bottom boundary layer flows Coastal Engineering. In *Proceedings of the 24th International Conference on Coastal Engineering Research Council* (pp. 384–398). Kobe, Japan.

Marani, M., D'Alpaos, A., Lanzoni, S., Carniello, L., & Rinaldo, A. (2007). Biologically controlled multiple equilibria of tidal landforms and the fate of the Venice lagoon. *Geophysical Research Letters*, *34*, L11402. https://doi.org/10.1029/2007GL030178

Marani, M., D'Alpaos, A., Lanzoni, S., Carniello, L., & Rinaldo, A. (2010). The importance of being coupled: Stable states and catastrophic shifts in tidal biomorphodynamics. *Journal of Geophysical Research*, *115*, F04004. https://doi.org/10.1029/2009JF001600

Marani, M., D'Alpaos, A., Lanzoni, S., & Santalucia, M. (2011). Understanding and predicting wave erosion of marsh edges. *Geophysical Research Letters*, *38*, L21401. https://doi.org/10.1029/2011GL048995

Mariotti, G., & Canestrelli, A. (2017). Long-term morphodynamics of muddy backbarrier basins: Fill in or empty out? *Water Resources Research*, *53*, 7029–7054. https://doi.org/10.1002/2017WR020461

Mariotti, G., & Carr, J. (2014). Dual role of salt marsh retreat: Long-term loss and short-term resilience. *Water Resources Research*, *50*, 2963–2974. https://doi.org/10.1002/2013WR014676

Mariotti, G., & Fagherazzi, S. (2010). A numerical model for the coupled long-term evolution of salt marshes and tidal flats. *Journal of Geophysical Research*, *115*, F01004. https://doi.org/10.1029/2009JF001326

Mariotti, G., & Fagherazzi, S. (2013a). Critical width of tidal flats triggers marsh collapse in the absence of sea-level rise. *Proceedings of the National Academy of Sciences*, *110*(14), 5353–5356. https://doi.org/10.1073/pnas.1219600110

Mariotti, G., & Fagherazzi, S. (2013b). Wind waves on a mudflat: The influence of fetch and depth on bed shear stresses. *Continental Shelf Research*, *60S*, S99–S110.

Marsooli, R., Orton, P. M., Georgas, N., & Blumberg, A. F. (2016). Three-dimensional hydrodynamic modeling of coastal flood mitigation by wetlands. *Coastal Engineering*, *111*, 83–94. https://doi.org/10.1016/j.coastaleng.2016.01.012

Marsooli, R., Orton, P. M., & Mellor, G. (2017). Modeling wave attenuation by salt marshes in Jamaica Bay, New York, using a new rapid wave model. *Journal of Geophysical Research: Oceans*, *122*, 5689–5707. https://doi.org/10.1002/2016JC012546

McFadden, L., Spencer, T., & Nicholls, R. J. (2007). Broad-scale modeling of coastal wetlands: What is required? *Hydrobiologia*, *577*(1), 5–15. https://doi.org/10.1007/s10750-006-0413-8

Mendez, F. M., & Losada, I. J. (2004). An empirical model to estimate the propagation of random breaking and nonbreaking waves over vegetation fields. *Coastal Engineering*, *51*, 103–118.

Miller, K. G., Kopp, R. E., Horton, B. P., Browning, J. V., & Kemp, A. C. (2013). A geological perspective on sea-level rise and impacts along the U.S. mid-Atlantic coast. *Earth's Future*, *1*, 3–18. https://doi.org/10.1002/2013EF000135

Morris, J. T., Barber, D. C., Callaway, J. C., Chambers, R., Hagen, S. C., Hopkinson, C. S., et al. (2016). Contributions of organic and inorganic matter to sediment volume and accretion in tidal wetlands at steady state. *Earth's Future*, *4*, 110–121. https://doi.org/10.1002/2015EF000334

Morris, J. T., Sundareshwar, P. V., Nietch, C. T., Kjerfve, B., & Cahoon, D. R. (2002). Responses of coastal wetlands to rising sea level. *Ecology*, *83*(10), 2869–2877. https://doi.org/10.1890/0012-9658(2002)083[2869:ROCWTR]2.0.CO;2

Nardin, W., Larsen, L., Fagherazzi, S., & Wiberg, P. (2018). Tradeoffs among hydrodynamics, sediment fluxes and vegetation community in the Virginia Coast Reserve, USA. *Estuarine, Coastal and Shelf Science*, *210*, 98–108. https://doi.org/10.1016/j.ecss.2018.06.009

New York City Department of Environmental Protection (2007). *Jamaica Bay watershed protection plan* (Vol. I). New York.

Orson, R., Panageotou, W., & Leatherman, S. P. (1985). Response of tidal salt marshes of the U.S. Atlantic and Gulf Coasts to rising sea levels. *Journal of Coastal Research*, *1*, 29–37.

Orton, P. M., Talke, S. A., Jay, D. A., Yin, L., Blumberg, A. F., Georgas, N., et al. (2015). Channel shallowing as mitigation of coastal flooding. *Journal of Marine Science and Engineering*, *3*(3), 654–673. https://doi.org/10.3390/jmse3030654

Pasternack, G. B., Hilgartner, W. B., & Brush, G. S. (2000). Biogeomorphology of an upper Chesapeake Bay river-mouth tidal freshwater marsh. *Wetlands*, *20*, 520–537. https://doi.org/10.1672/0277-5212(2000)020<0520:BOAUCB>2.0.CO;2

Pawlowicz, R., Beardsley, B., & Lentz, S. (2002). Classical tidal harmonic analysis including error estimates in MATLAB using T_TIDE. *Computational Geosciences*, *28*(8), 929–937. https://doi.org/10.1016/S0098-3004(02)00013-4

Peteet, D. M., Nichols, J., Kenna, T., Chang, C., Browne, J., Reza, M., et al. (2018). Sediment starvation destroys New York City marshes' resistance to sea level rise. *Proceedings of the National Academy of Sciences*, *115*(41), 10,281–10,286. https://doi.org/10.1073/pnas.1715392115

Ralston, D. K., Geyer, W. R., & Warner, J. C. (2012). Bathymetric controls on sediment transport in the Hudson River estuary: Lateral asymmetry and frontal trapping. *Journal of Geophysical Research*, *117*, C10013. https://doi.org/10.1029/2012JC008124

Reed, D. J. (1995). The response of coastal marshes to sea-level rise: Survival or submergence? *Earth Surface Processes and Landforms*, *20*(1), 39–48. https://doi.org/10.1002/esp.3290200105

Renfro, A., Cochran, J., Hirschberg, D., Bokuniewicz, H., & Goodbred, S. (2016). The sediment budget of an urban coastal lagoon (Jamaica Bay, NY) determined using ^{234}Th and ^{210}Pb. *Estuarine, Coastal and Shelf Science*, *180*, 136–149. https://doi.org/10.1016/j.ecss.2016.06.008

Renfro, A., Cochran, J., Hirschberg, D., & Goodbred, S. (2010). Natural Radionuclides (^{234}th, ^{7}be and ^{210}pb) as Indicators of Sediment Dynamics in Jamaica Bay, New York. Natural Resource Technical Report NPS/NERO/NRTR—2010/324. Fort Collins, CO.

Schwimmer, R. (2001). Rates and processes of marsh shoreline erosion in Rehoboth Bay, Delaware, U.S.A. *Journal of Coastal Research*, *17*(3), 672–683. https://doi.org/10.1016/j.csr.2009.08.018

Shchepetkin, A. F., & McWilliams, J. C. (2005). The Regional Ocean Modeling System: A split-explicit, free-surface, topography following coordinates ocean model. *Ocean Modelling*, *9*(4), 347–404. https://doi.org/10.1016/j.ocemod.2004.08.002

Stevenson, J. C., Kearney, M. S., & Pendleton, E. C. (1985). Sedimentation and erosion in a Chesapeake Bay brackish marsh system. *Marine Geology*, *67*(3–4), 213–235. https://doi.org/10.1016/0025-3227(85)90093-3

Swanson, R. L., & Wilson, R. E. (2008). Increased tidal ranges contribute to marsh flooding. *Journal of Coastal Research*, *24*, 1565–1569.

Talke, S. A., & Jay, D. A. (2020). Changing tides: The role of natural and anthropogenic factors. *Annual Review of Marine Science*, *12*(1), 121–151. https://doi.org/10.1146/annurev-marine-010419-010727

Tambroni, N., & Seminara, G. (2012). A one-dimensional eco-geomorphic model of marsh response to sea level rise: Wind effects, dynamics of the marsh border and equilibrium. *Journal of Geophysical Research*, *117*, F03026. https://doi.org/10.1029/2012JF002363

Tommasini, L., Carniello, L., Ghinassi, M., Roner, M., & D'Alpaos, A. (2019). Changes in the wind-wave field and related salt-marsh lateral erosion: Interferences from the evolution of the Venice Lagoon in the last four centuries. *Earth Surface Processes and Landforms*, *44*(8), 1633–1646. https://doi.org/10.1002/esp.4599

Tonelli, M., Fagherazzi, S., & Petti, M. (2010). Modeling wave impact on salt marsh boundaries. *Journal of Geophysical Research*, *115*, C09028. https://doi.org/10.1029/2009JC006026

Uittenbogaard, R. (2003). Modelling turbulence in vegetated aquatic flows. *In International workshop on Riparian Forest vegetated channels: Hydraulic, morphological and ecologic al aspects, 20–22 February 2003*. Trento, Italy.

Van der Wegen, M., Dastgheib, A., & Roelvink, J. (2010). Morphodynamic modeling of tidal channel evolution in comparison to empirical PA relationship. *Coastal Engineering*, *57*, 827–837.

Vermeulen, T. J. (2003). Sensitivity analysis of fine sediment transport in the Humber estuary, Masters, Delft University of Technology.

Warner, J. C., Armstrong, B., He, R., & Zambon, J. B. (2010). Development of a Coupled Ocean-Atmosphere-Wave-Sediment Transport (COAWST) modeling system. *Ocean Modelling*, *35*(3), 230–244. https://doi.org/10.1016/j.ocemod.2010.07.010

Warner, J. C., Sherwood, C. R., Signell, R. P., Harris, C., & Arango, H. G. (2008). Development of a three-dimensional, regional, coupled wave, current, and sediment-transport model. *Computers and Geosciences*, *34*(10), 1284–1306. https://doi.org/10.1016/j.cageo.2008.02.012

Wigand, C., Roman, C. T., Davey, E., Stolt, M., Johnson, R., Hanson, A., et al. (2014). Below the disappearing marshes of an urban estuary: Historic nitrogen trends and soil structure. *Ecological Applications*, *24*(4), 633–649. https://doi.org/10.1890/13-0594.1

Zhang, X., Leonardi, N., Donatelli, C., & Fagherazzi, S. (2019). Fate of cohesive sediments in a marsh-dominated estuary. *Advances in Water Resources*, *125*, 32–40. https://doi.org/10.1016/j.advwatres.2019.01.003